AUTOPHAGY
2022, VOL. 18, NO. 12, 3023–3030
https://doi.org/10.1080/15548627.2022.2054241

Taylor & Francis
Taylor & Francis Group

ADDENDUM

ATG16L1 WD40 domain-dependent IL10R (interleukin 10 receptor) signaling is insensitive to the T300A Crohn disease risk polymorphism

Inmaculada Serramito-Gómez, Elena Terraza-Silvestre*, Álvaro Fernández-Cabrera*, Raquel Villamuera, and Felipe X. Pimentel-Muiños†

Instituto de Biología Molecular y Celular del CáncerCentro de Investigación del Cáncer, Consejo Superior de Investigaciones Científicas (CSIC)-Universidad de Salamanca, Campus Miguel de Unamuno, Salamanca, Spain

ABSTRACT

A coding allele of *ATG16L1* that increases the risk of Crohn disease (T300A; rs2241880) impairs the interaction between the C-terminal WD40 domain (WDD) and proteins containing a WDD-binding motif, thus specifically inhibiting the unconventional autophagic activities of ATG16L1. In a recent publication we described a novel atypical role of ATG16L1 in the regulation of IL10R (interleukin 10 receptor) trafficking and signaling, an activity that involves direct interaction between the WDD and a target motif present in IL10RB (interleukin 10 receptor subunit beta). Here we show that, unexpectedly, neither the ability of ATG16L1 to interact with IL10RB nor its role in supporting IL10 signaling are altered by the T300A mutation. These results indicate that the ATG16L1^{T300A} allele selectively impairs the interaction between the WDD and a subset of WDD-binding motif versions, suggesting that only a fraction of the unconventional activities mediated by ATG16L1 are required to prevent Crohn disease.

Abbreviations: ATG, autophagy related; ATG16L1, autophagy related 16 like 1; BMDMs, bone marrow-derived macrophages; CRISPR, clustered regularly interspaced short palindromic repeats; CSF1/M-CSF, colony stimulating factor 1; FBS, fetal bovine serum; GSH, glutathione; IL10, interleukin 10; IL10R, interleukin 10 receptor; LPS, lipopolysaccharide; MAP1LC3/LC3, microtubule associated protein 1 light chain 3; MEFs, mouse embryonic fibroblasts; PMA, phorbol myristate acetate; p-STAT3: phosphorylated STAT3; qPCR, quantitative polymerase chain reaction; SDS, sodium dodecyl sulfate; sgRNA, single guide RNA; TMEM59, transmembrane protein 59; TNF, tumor necrosis factor; TNFAIP3/A20, TNF alpha induced protein 3; WDD, WD40 domain; WIPI2, WD repeat domain, phosphoinositide interacting 2

ARTICLE HISTORY
Received 11 January 2022
Revised 11 March 2022
Accepted 14 March 2022

KEYWORDS
ATG16L1; crohn disease; cytokine signaling; T300A allele; unconventional autophagy; WD40 domain

Introduction

ATG16L1 is a critical mediator of macroautophagy (hereafter referred to as autophagy) that plays an important role in the MAP1LC3/LC3 lipidation complex [1], both as a scaffold for the macromolecular assembly and also by specifying the membrane site where LC3 will be lipidated [2]. ATG16L1 includes a large C-terminal domain formed by 7 WD40-type repeats (WD40 domain, WDD, residues 320–607) [3] whose function has remained unclear. This is because a version of ATG16L1 lacking this region is fully competent to sustain canonical autophagy in mammalian cells [4–6], leading to the idea that the WD40 repeats are irrelevant for the canonical autophagic pathway. Recent studies have revealed that the WDD is critical for unconventional autophagic activities where LC3 becomes lipidated in single-membrane intracellular compartments unrelated to canonical double-membrane autophagosomes [5–7], like for example vesicles of the endosomal (LC3-associated endocytosis, LANDO) [8] or phagosomal (LC3-associated phagocytosis, LAP) [6] compartments. Conjugation of LC3 to single membranes/CASM in response to lysosomotropic drugs [6,9] or *Salmonella* infection [10] is also mediated by the WDD through the vacuolar-type H^+-translocating ATPase (V-ATPase). The physiological implications of these unconventional processes are beginning to be unraveled.

We previously found that the ATG16L1 WDD provides a docking surface for molecules that contain a specific WDD-binding amino acid motif, an interaction that allows engagement of the LC3 lipidation activity of the N-terminal domain in unconventional localizations [7,11]. We originally discovered the WDD-binding motif in the intracellular domain of the transmembrane protein TMEM59, where its ability to recruit ATG16L1 causes labeling of the same endosomes where TMEM59 is located with LC3 to promote their targeting to the lysosomal compartment [7]. Since then, we found that the ubiquitin editor and anti-inflammatory mediator TNFAIP3/A20 includes a similar WDD-binding element [12], and we also identified IL10RB as a protein able to bind the WDD through a motif present in its intracellular region [13]. In this case, the interaction between IL10RB and the WDD is required for proper endocytosis, early trafficking and

CONTACT Felipe X. Pimentel-Muiños fxp@usal.es;fxp@cbm.csic.es Instituto de Biología Molecular y Celular del Cáncer. Centro de Investigación del Cáncer, Centro de Biología Molecular Severo Ochoa (CSIC-UAM), Nicolás Cabrera, 1. Salamanca, Madrid, 28049, Spain
†Present Address: Centro de Biología Molecular Severo Ochoa (CSIC-UAM)
*These authors contributed equally to this work

optimal signaling output of the receptors upon engagement by IL10 [13]. Because yeast Atg16 lacks the WDD, the evolutionary addition of this domain has likely facilitated extension of ATG16L1 functions to specialized activities that may be exclusive of multicellular organisms.

A coding polymorphic allele of *ATG16L1* that changes Thr to Ala at position 300 (T300A; rs2241880) increases the risk of suffering Crohn disease [14,15], an intestinal inflammatory pathology that is currently incurable [16]. Previous data suggest that the T300A allele impairs the unconventional functions of ATG16L1 without influencing canonical autophagy [5]. For instance, secretion of anti-microbial peptides by Paneth cells [17], the control of innate immune inflammatory responses [18] or some anti-bacterial defense mechanisms [19,20] are all impaired by ATG16L1^{T300A}. Mechanistically, the T300A mutation has been shown to increase susceptibility of an overlapping target site to caspase processing [20,21], and also to decrease the ability of the WDD to bind the WDD-binding motif present in TMEM59 under healthy conditions where caspase activity is minimal [5]. This latter defect alters the intracellular trafficking and normal function of TMEM59, thus impairing the innate cellular defense against bacterial infections [5]. Given that the T300A mutation inhibits the ability of the WDD to interact with its target motif in TMEM59, we hypothesized that the interaction between ATG16L1 and IL10RB that we recently reported [13] could also be inhibited by the T300A allele. IL10 is a prominent anti-inflammatory cytokine [22], so defective IL10R signaling caused by ATG16L1^{T300A} could explain at least part of the pro-inflammatory consequences of the T300A mutation.

Here we show that, contrary to what we expected, the T300A mutation did not impair neither the WDD-dependent interaction between ATG16L1 and IL10RB nor the functional properties of IL10RB, suggesting that only a fraction of WDD-binding motif-containing proteins may be susceptible to the deleterious effects of this allele.

Results

To explore if the T300A mutation impedes the interaction between ATG16L1 and IL10RB we confronted tagged versions of the receptor with wild-type (WT) ATG16L1 (T300) and ATG16L1^{T300A} (A300) forms of ATG16L1 (isoform β) in co-immunoprecipitation assays carried out in HEK-293 T cells, following the same protocols we used in our previous publication [13]. Surprisingly, IL10RB bound equally well to both constructs (Figures 1A and 1B), indicating that the T300A mutation has no obvious impact on the ability of the WDD to recognize its target motif in IL10RB. This result is in contrast to previous data showing that the WDD of ATG16L1^{T300A} interacts defectively with TMEM59 [5] (see also Figure 1A, bottom panel), but is consistent with other data indicating that TNFAIP3/A20 binds ATG16L1^{T300A} normally [12].

While the T300A mutation prevents the interaction between the WDD and TMEM59, whether or not it might have additional consequences in the ability of ATG16L1 to relay downstream unconventional autophagic signals is unclear. Since IL10RB interacts with the WDD in a T300A-insensitive manner it constitutes a good system to test this idea, so we carried out a variety of functional studies to explore if IL10R signaling might be influenced by the T300A allele. To this end, we engineered *atg16l1*$^{-/-}$ mouse embryonic fibroblasts (MEFs) to express T300 or A300 ATG16L1β cDNAs from a retroviral vector, and we subsequently reconstituted both cellular strains with the critical elements of the IL10R signaling system: STAT3, a STAT3-luciferase transcriptional reporter and both IL10 receptors, as we have done in our previous studies [13]. ATG16L1 transgene expression levels were comparable in T300 and A300 strains (Figure 2A) and, consistent with previous publications [5], both the basal (Figure 2B, left panel) and rapamycin-induced (Figure 2B, right panel) canonical autophagic fluxes remained unaltered in A300-expressing cells. In addition, the expression levels of IL10Rs (A and B chains) were similar in WT ATG16L1 and ATG16L1^{T300A} cells, measured by both western blotting (Figure 2C) and flow cytometry (Figure 2D), thus allowing direct comparison of IL10 signaling between both cellular systems. Consistent with the data mentioned above (see Figures 1A and 1B), co-immunoprecipitation studies carried out upon IL10 exposure in the same conditions we previously optimized for specific binding [13] showed the same levels of WT ATG16L1 and ATG16L1^{T300A} in IL10RB-Flag immunoprecipitates (Figure 2E), and comparable IL10RB signals present in WT HA-ATG16L1 and HA-ATG16L1^{T300A} precipitates (Figure 2F). These results are again consistent with the idea that the T300A mutation does not impair the IL10RB-ATG16L1 interaction in response to IL10 stimulation. Signaling studies performed in these cells using the STAT3-luciferase reporter system indicated that IL10 signaling remains unaltered in cells expressing ATG16L1^{T300A} (Figure 2G), under the same experimental settings established in our previous article to observe the effect of the WDD [13].

To explore this issue in cells naturally responsive to IL10, we resorted to the THP1 human monocytic cell line, which becomes strongly sensitive to IL10 after phorbol myristate acetate (PMA) treatment [13]. Endogenous ATG16L1 was depleted in these cells using a lentiviral version of the CRISPR-Cas9 system, and we subsequently restored the depleted strain with single guide RNA (sgRNA)-resistant, silent mutants of WT ATG16L1β or ATG16L1β^{T300A}. The expression levels of both ATG16L1 versions were comparable in both engineered cell lines (Figure 3A). Consistent with the results observed in MEFs, IL10 induced similar levels of nuclear phosphorylated STAT3 (p-STAT3) measured at different times post-treatment in both WT ATG16L1 and ATG16L1^{T300A} cells (Figure 3B), arguing again that IL10 signaling is unaffected in A300-expressing cells. Last, to verify these results in primary cells, we isolated bone marrow-derived macrophages (BMDMs) from wild-type and knock-in mice expressing the T300A mutation [20], confirmed that they express comparable levels of ATG16L1 (Figure 3C) and subjected them to a variety of IL10 signaling studies. We found that IL10 was able to induce similar levels of nuclear p-STAT3 (Figure 3D), comparable expression of *Bcl3* (an IL10-responsive gene; Figure 3E) and equal suppression of *Tnf/TNFα* mRNA induction by lipopolysaccharide (LPS; Figure 3F) in T300 and A300 BMDMs.

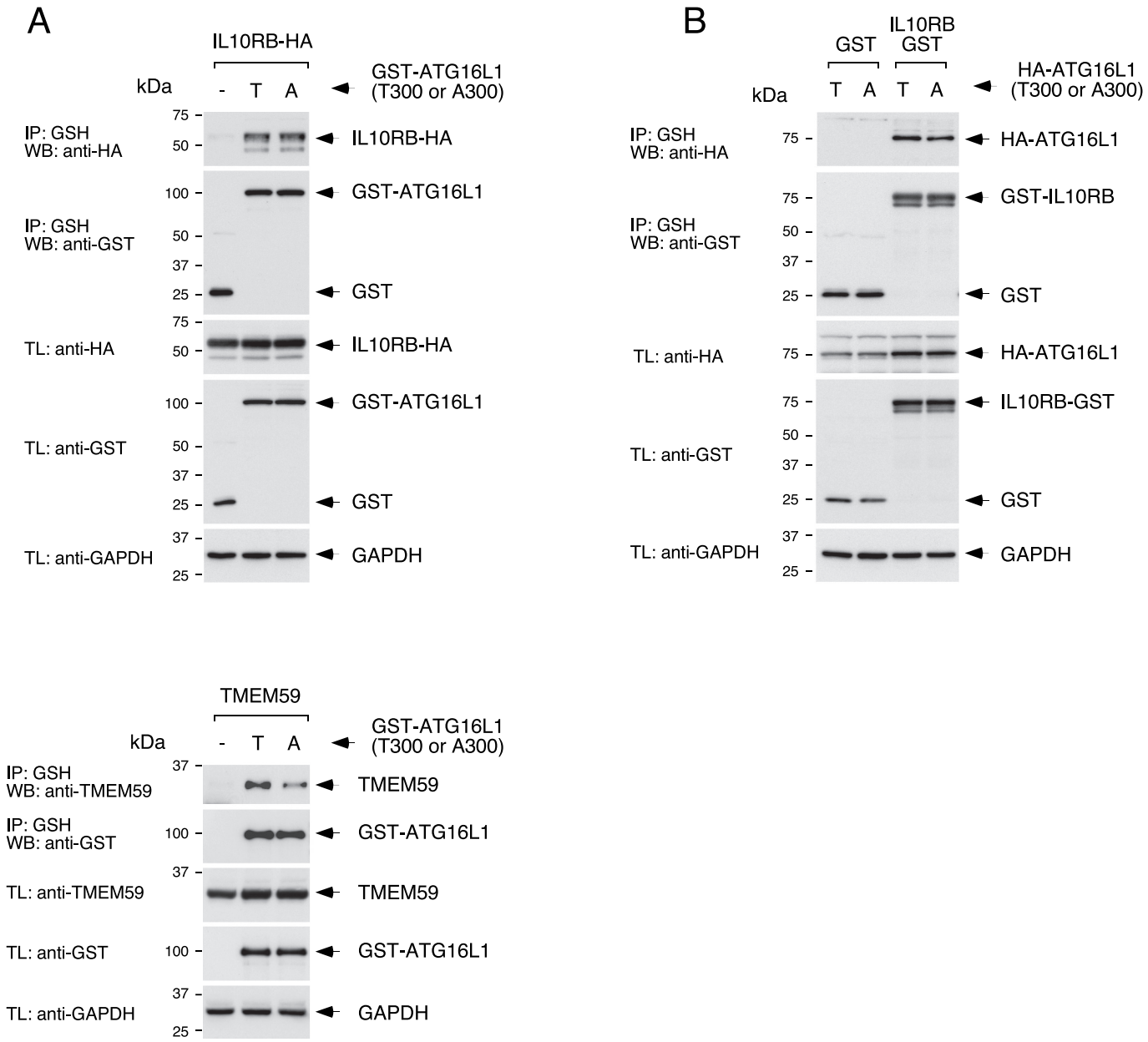

Figure 1. Comparable interaction between IL10RB and WT ATG16L1β (T300, T) or ATG16L1β^{T300A} (A300, A). HEK-293 T cells were co-transfected with the indicated constructs, lysed 36 h later and subjected to GST immunoprecipitation with agarose beads coupled to GSH. Shown are western blots against the indicated molecules. IP: immunoprecipitate; TL: total lysate. (A) Co-immunoprecipitation between GST-ATG16L1β or GST-ATG16L1β^{T300A} and IL10RB-HA (top panel) or TMEM59 (bottom panel). (B) Co-immunoprecipitation between GST-IL10RB and HA-ATG16L1β or HA-ATG16L1β^{T300A}.

Discussion

We previously showed that the T300A mutation inhibits the ability of the WDD to bind its target motif present in TMEM59, so we hypothesized that all molecules including a functional WDD-binding motif might be unable to properly recognize ATG16L1^{T300A}. Unexpectedly however, we found that at least in the case of IL10RB, this is not the case, as its interaction with ATG16L1^{T300A} remains unaltered. We also established that none of the main functional consequences of ATG16L1 in IL10RB biology are affected by the T300A mutation, indicating that ATG16L1^{T300A} fully retains the potential to relay downstream unconventional autophagic signals provided that binding to the upstream motif-containing inducer is unaffected.

These results have important implications regarding the molecular consequences that the T300A mutation has in the biology of ATG16L1. First, it appears that, in the absence of significant caspase activity and proteolysis of ATGL6L1, only a fraction of motif-containing WDD-binding molecules show defective binding to ATG16L1^{T300A}, thus pointing to the interesting idea that the T300A mutation alters the function of a limited set of WDD-interacting molecules under healthy conditions. As we recently established [13], the WDD-binding motif is complex, with a number of positions being quite flexible, so it is possible that different versions of the motif may show different affinities for the T300 and A300 ATG16L1 forms. This scenario is consistent with the idea that the T300A mutation may cause a mild structural

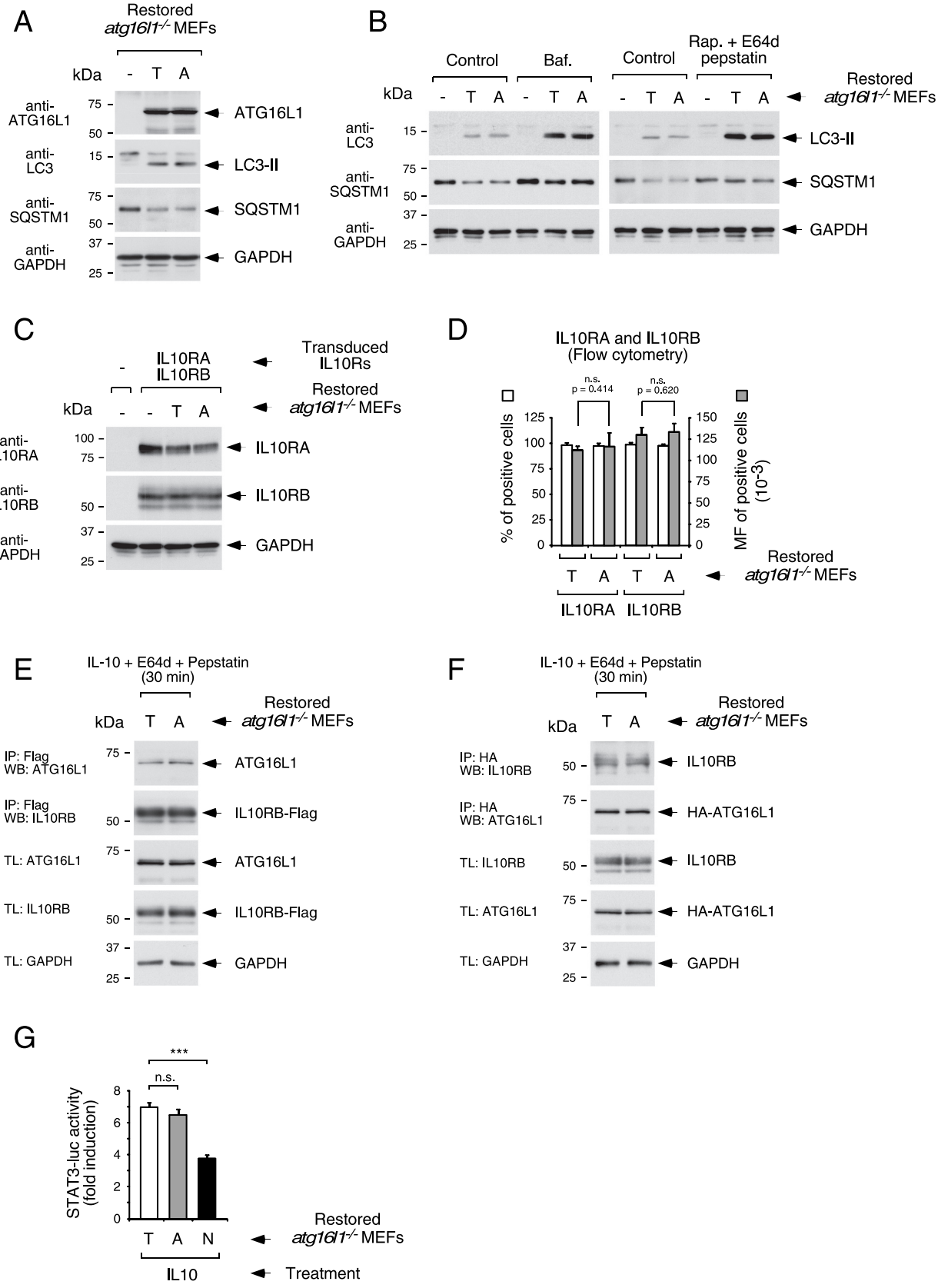

Figure 2. Unaltered IL10R signaling in MEFs expressing ATG16L1^{T300A}. *atg16l1*$^{-/-}$ MEFs were retrovirally transduced to harbor a STAT3-luciferase reporter system and to express STAT3, WT ATG16L1β (T300) or ATG16L1β^{T300A} constructs (T or A, respectively), and IL10Rs A and B. (A) Expression levels of WT ATG16L1 and ATG16L1^{T300A}. Cells were lysed for western blotting against the indicated molecules. (B) Autophagic flux in cells expressing ATG16L1β or ATG16L1β^{T300A}. The indicated cells were treated with bafilomycin A_1 (Baf., 75 nM, 6 h; left panel) or rapamycin (Rap.), E64d and pepstatin (2 μM and 10 μg/ml each, respectively, for 10 h; right panel), and lysed for western blotting. (C) IL10RA and IL10RB expression in the engineered MEFs. Cells were lysed for the indicated western blots. (D) Surface expression levels of IL10Rs. Cells were subjected to flow cytometry with specific anti-IL10R antibodies. Shown are average percentages of positive cells with respect to control cells lacking IL10Rs (left axis, white bars) and the average mean of fluorescence of the positive cells (MF, right axis, gray bars), from triplicate experimental

alteration to the WDD that modifies the specificity of the interaction between full-length, uncleaved ATG16L1 and its natural ligands, rather than completely disrupting the interaction capabilities of the WDD [5,23]. A bipartite membrane-binding region spanning position 300 in ATG16L1β (amino acids 266–319) has been shown to be important for LC3 lipidation at high, but not low, curvature vesicles [24]. Assuming that the T300A mutation could disturb this membrane-binding region, it is conceivable that a possible different size and/or curvature of the endosomal vacuoles carrying TMEM59 or IL10RB could contribute to the differential effect of the T300A mutation on the function of both effectors.

Second, since IL10RB functions normally in the presence of ATG16L1^{T300A}, the T300A mutation is unlikely to have additional functional consequences in the atypical activities of ATG16L1 other than disrupting the interaction features of the WDD. Thus, its ability to promote LC3 lipidation or to interact with other effectors that bind the N-terminal domain (ATG5, RB1CC1/FIP200, WIPI2, RAB33) likely remain unaffected, also explaining why ATG16L1^{T300A} can fully sustain the canonical autophagic pathway. Consequently, systematic identification of the specific set of motif-containing proteins showing defective interaction with ATG16L1^{T300A} will likely lead to the relevant molecules and their associated biological activities whose normal function is required prevent the onset of Crohn disease. Whether this is a large set of proteins or if TMEM59 is the main effector whose dysfunction by ATG16L1^{T300A} explains the pathological effects of the T300A mutation is currently unclear, but this is a relevant question that we believe is worth exploring.

Third, while these considerations apply to healthy conditions with minimal caspase activity, the T300A mutation may derail the normal function of all WDD interactors in physiological situations accompanied by elevated caspase function. In such apoptotic scenario, caspase processing of ATG16L1^{T300A} would uncouple the Nt and Ct (WDD) domains, thus inhibiting the ability of WDD-interacting proteins to induce the LC3-lipidation activity of the N-terminal domain in unconventional localizations.

Identification of the whole collection of motif-containing, WDD-interacting proteins and establishing the specific fraction of this collection that binds defectively to ATG16L1^{T300A} will help increase our understanding of the physiological dysfunctions that are caused by this allele to increase the risk of Crohn disease and other pathologies.

Materials and methods

Cell lines, cell culture and reagents

HEK-293T and THP1 cells were obtained from the American Type Culture Collection (CRL-11268 and TIB-202, respectively). The *atg16l1*$^{-/-}$ MEFs were described previously [25,26], and we engineered these cell by transducing them first with a retroviral STAT3-luciferase reporter system and a plasmid expressing human STAT3. Cells were then restored with retroviral constructs expressing WT ATG16L1β (T300) or ATG16L1β^{T300A} (A300) forms. Finally, cells were transduced with a mixture of retroviral supernatants harboring human IL10RA-AU and IL10RB-Flag. THP1 cells were infected with lentiviruses expressing the CRISPR-Cas9 guide against *ATG16L1* and selected in puromycin (1 µg/ml; Sigma, P8833) for 6–7 days. Cells were then restored via retroviral transduction of constructs expressing WT ATG16L1β or ATG16L1β^{T300A} where the sgRNA target sequence was silently inactivated by mutation. Cells were cultured at 37°C and a humidified 5% CO_2 atmosphere, in DMEM (Invitrogen, 41966052) supplemented with 10% heat-inactivated fetal bovine serum (FBS; Invitrogen, 10270106), 2 mM glutamine and 100 U/ml of penicillin-streptomycin (Invitrogen, 15140130). Bafilomycin A_1, pepstatin and rapamycin were purchased from Sigma (B1793, P4265, R0395, respectively), and E64d from Calbiochem (330005). Recombinant human and mouse IL10 and CSF1/M-CSF were from Life Technologies (PHC0105), R&D (417-ML-005) and Biolegend (574804). For pulse-chase experiments, cells were incubated with IL10 for 30 min at 4°C, washed twice and incubated at 37°C for the relevant times before lysis for western blotting.

DNA constructs

All constructs for cDNA expression were cloned into the pEAK series of mammalian expression vectors (kind gift by Dr. Brian Seed, MGH, Boston, MA, US) or a retroviral derivative called P12-MMP (kind gift by Dr. Felix Randow, LMB, Cambridge, UK). The *ATG16L1* cDNA isoform used in all experiments was *ATG16L1*β. For experiments involving the CRISPR-Cas9 system to deplete ATG16L1 in human THP1 cells, the specific sgRNA guide was cloned using suitable BsmBI restriction sites available in the lentiviral vector lentiCRISPRv2 that also expresses Cas9 and the puromycin resistance gene (Addgene, 52961; deposited by Dr. Feng Zhang). The guide is directed to positions 78–97 of the *ATG16L1* mRNA (5' GCTGCAGAGACAGGCGTTCG 3', counting from the first coding nucleotide in the *ATG16L1* mRNA) and was selected using the BreakingCas server at the Centro Nacional de Biotecnología (Madrid, Spain; https://bioinfogp.cnb.csic.es/tools/breakingcas/index.php). Once ATG16L1 was successfully depleted, cells were restored via retroviral transduction of constructs expressing WT ATG16L1β or ATG16L1β^{T300A} versions where the sgRNA target sequence and the PAM were silently mutated using the oligonucleotide: 5' GCT**c**CAGAG**g**CA**a**GC**c**TTCGA**a**G 3'.

points -/+ s.d. (n = 3; n.s. *P*-value > 0.05, two-sided Student's *t*-test). (E) Unaltered binding of HA-ATG16L1^{T300A} to IL10RB-Flag upon IL10 exposure. The indicated cells expressing T or A alleles of ATG16L1β, IL10RA and IL10RB-Flag were treated with IL10 (50 ng/ml) in the presence of E64d and pepstatin (10 µg/ml each) for 30 min and lysed for anti-Flag immunoprecipitation. The resulting precipitates were subjected to western blotting. (F) Comparable levels of IL10RB in HA-ATG16L1 or HA-ATG16L1^{T300A} immunoprecipitates upon IL10 treatment. The same cells as in E were treated as in E and subjected to anti-HA immunoprecipitation for western blotting. The experimental conditions used in E and F provide specific co-precipitation signals as established in our previous publication [13]. (G) Similar IL10-induced signaling in cells expressing ATG16L1 or ATG16L1^{T300A}. The indicated cells (N, cells expressing ATG16L1 N-terminal domain; residues 1–299) were treated with IL10 (4 h, 50 ng/ml) and lysed to measure luciferase activity. Data show means of fold induction of luciferase activity -/+ s.d. (n = 3; n.s.: $P > 0.05$; (***); $P < 0.001$, two-sided Student's *t*-test).

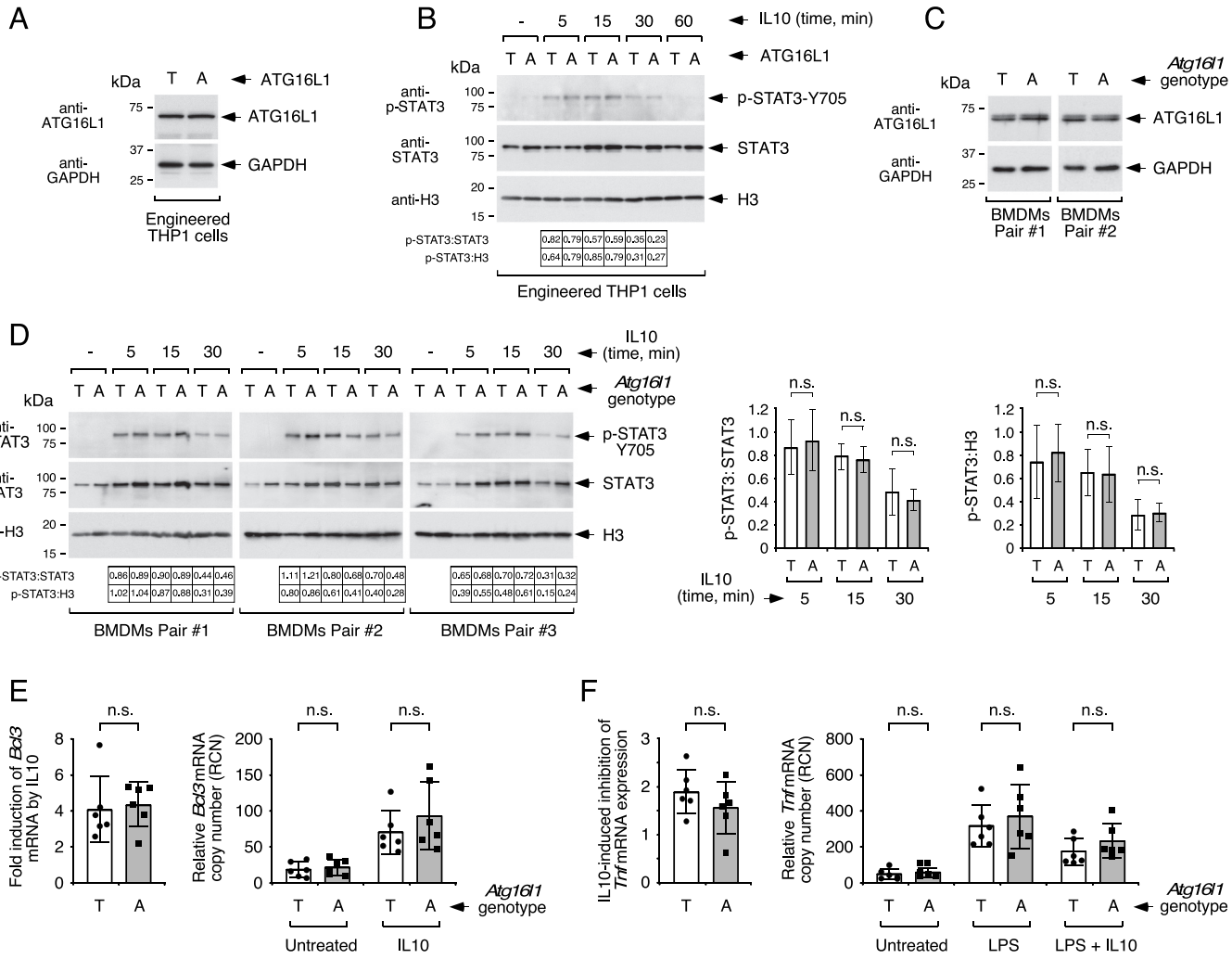

Figure 3. Unaltered IL10 signaling in THP1 cells and BMDMs expressing ATG16L1^{T300A}. (A) ATG16L1 expression levels in THP1 cells depleted of endogenous ATG16L1 and restored with sgRNA-resistant versions of WT ATG16L1β or ATG16L1β^{T300A}. The indicated cells were lysed for western blotting against the shown molecules. (B) Pulse-chase assay of IL10-induced nuclear phosphorylated STAT3 (p-STAT3) in THP1 cells. Cells described in A were treated with PMA (125 ng/ml; 48 h), incubated with IL10 (50 ng/ml) for the indicated times following a pulse-chase protocol, and lysed to obtain nuclear extracts for the indicated western blots. Corrected densitometric quantifications are shown at the bottom of the western blot panels. This experiment was repeated twice with similar results. (C) Expression levels of ATG16L1 in BMDMs isolated from WT *Atg16l1* and *Atg16l1*^{T300A} mice. Bone marrow cells were isolated from the indicated mice, differentiated in the presence of CSF1 (20 ng/ml; 6 days) and lysed for western blotting. (D) Pulse-chase assay of IL10-induced p-STAT3 phosphorylation in BMDMs. BMDMs isolated as in C from 3 randomly-chosen mice pairs were treated with IL10 (50 ng/ml) for the indicated times and lysed to obtain nuclear extracts for western blot. Corrected densitometric quantifications are shown at the bottom. Graphs on the right include statistics of the obtained densitometry values (n = 3; (n.s.): $P > 0.05$, two-sided Student's *t*-test). (E) Quantitative PCR to evaluate IL10-induced *Bcl3* expression. BMDMs were obtained as in C, treated with IL10 (50 ng/ml, 4 h) and lysed for *Bcl3* qPCR. Data are expressed as average fold-inductions caused by IL10 treatment -/+ s.d. (n = 6 mice; (n.s.): $P > 0.05$, two-sided Student's *t*-test; left panel), and relative copy number (RCN) for the individual samples (right panel). (F) Quantitative PCR to assess IL10-induced suppression of *Tnf* mRNA upregulation by LPS. BMDMs were isolated as in C, treated with LPS (1 ng/ml; 6 h) with or without IL10 (50 ng/ml) and lysed for *Tnf* qPCR. Data are expressed as average fold-inhibition values caused by IL10 -/+ s.d. (n = 6 mice; (n.s.): $P > 0.05$, two-sided Student's *t*-test; left panel), and relative copy numbers (RCNs, right panel).

ATG16L1β including the T300A mutation was generated by site-directed mutagenesis using a mutagenic oligonucleotide: 5' CAGGACAATGTGGAT**g**CTCATCCTGGTTCTGG 3' and verified by sequencing. Constructs expressing HA- and GST-tagged human ATG16L1β, IL10RB-Flag, -HA or -GST, IL10RA-AU, STAT3, STAT3-luciferase were described previously [13].

Transfections and viral transductions

Transfections were carried out using jetPEI (Polyplus, 101–40). Retroviral transductions were carried out using viral supernatants generated by co-transfecting the relevant P12-MMP constructs into HEK-293 T cells together with helper plasmids expressing gag-pol (pMD.gag-pol) and env (VSV-G; pMD-G), both kindly shared with us by Dr. Richard Mulligan (Harvard University, Boston, MA, US). Viral supernatants were collected 48 h post-transfection, diluted 1:1 with fresh medium supplemented with 8 µg/ml polybrene (Sigma, H9268), and spun onto the target cells for 1 h, 850 x g, 32°C. To perform lentiviral transductions to deplete ATG16L1 in THP1 cells using the CRISPR-Cas9 system, we co-transfected the lentiCRISPRv2 plasmid along with the helper plasmids psPAX2 (Addgene, 12260; deposited by Dr. Didier Trono) and pCMV-VSV-G

(Addgene, 8454; deposited by Dr. Robert Weinberg) into HEK-293T cells. Viral supernatants were diluted 4:1 with fresh medium and used to infect the target cells essentially as described above for retroviral transductions.

Cell lysis, western blotting and co-precipitation studies

Total cell lysates were isolated by resuspending the cell pellets in 2x sodium dodecyl sulfate (SDS) sample buffer (SB) lacking β-mercaptoethanol and bromophenol blue (100 mM Tris-HCl, pH 6.8, 4% SDS and 20% glycerol) but supplemented with PMSF (10 µg/ml; Roche, 837,091) and a protease inhibitor cocktail (Sigma, P8340). Samples were boiled for 15 min and spun for 5 min remove debris. To generate nuclear extracts, cells were lysed on ice for 30 min in a buffer containing 1% Igepal CA-630 detergent (Sigma, I3021), 150 mM NaCl, 50 mM Tris, pH 7.5, 5 mM EDTA, protease inhibitors (PMSF and protease inhibitor cocktail) and phosphatase inhibitors β-glycerophosphate (25 mM; Sigma, G9422), sodium fluoride (5 mM; Sigma, S7920) and orthovanadate (1 mM; New England Biolabs, P0758) and centrifuged at 16,100 x g for 10 min. The resulting nuclear pellets were lysed in SB as described above. Protein concentrations were obtained using the DC Protein Assay (Bio-Rad, 5000116). For co-immunoprecipitation assays, cells were lysed in the same buffer as above and the resulting lysates diluted 1:5 to a final detergent concentration of 0.2%. Lysates were then pre-cleared with agarose beads (1 h, 4°C, rotation; Sigma, 4B200) and immunoprecipitated with the relevant primary antibodies (3 h, 4°C, rotation) plus agarose beads coupled to protein G (1 h, 4°C, rotation; GE Healthcare, 17–0618-01), or agarose beads coupled to glutathione (GSH, 3 h, 4°C, rotation; GE Healthcare, 17–0756-01). Immunoprecipitating antibodies: Anti-Flag (D6W5B, rabbit; Cell Signaling Technology, 14,793; 1:150) or anti-HA (16B12, mouse, BioLegend 901501, 1:150). Beads were washed 3–4 times with cold immunoprecipitation buffer (0.2% detergent), resuspended in 2x Reducing Sample buffer, and boiled for 10 min. Equal amounts of protein or immunoprecipitation eluates were resolved by SDS-PAGE, transferred to a polyvinilidene difluoride membrane (Millipore, IPVH00010) and probed with primary antibodies against GST (rabbit; Cell Signaling Technology, 2622), HA (16B12, mouse, Babco Biolegend, 901501; or C29F4, rabbit, Cell Signaling Technology, 3724S), Flag (M2, mouse, Sigma F3165; or D6W5B, rabbit, Cell Signaling Technology, 14793), GFP (B34, mouse; BioLegend, 902601), ATG16L1 (1F12, mouse, MBL, M150-3 or rabbit, PM040), IL10RA (A3, mouse; Santa Cruz Biotechnology, sc-365,374), IL10RB (F6, mouse; Santa Cruz Biotechnology, sc-271969), TMEM59 (generated in-house, rabbit polyclonal), phosphorylated STAT3-Y705 (rabbit; Cell Signaling Technology, 9131), STAT3 (mouse; Cell Signaling Technology, 9139), Histone H3 (D1H2, rabbit mAb; Cell Signaling Technology, 4499), LC3 (mouse; MBL, M186-3), SQSTM1/p62 (mouse; BD, 610833), GAPDH (6C5, mouse; Abcam, ab8245). Blots were incubated with the appropriate secondary HRP-coupled antibodies (Jackson Immunoresearch, anti-mouse, 115–035-003; anti-rabbit, 111–035-003) and developed by chemiluminescence (ECL; Amersham, RPN2134).

Flow cytometry

MEFs were resuspended in culture medium supplemented with 0.1% azide and mouse immunoglobulins (1:100; Sigma, 12–371), and pre-incubated for 30 min on ice. Cells were then incubated with the specific antibodies (1:100, 30 min, ice) with occasional gentle mixing, washed and analyzed in an Accuri C6 (BD BioSciences) flow cytometer. Specific antibodies were: anti-human-IL10RA-Alexa Fluor 647 (rat; BD, 565255), anti-human-IL10RB-Alexa Fluor 647 (mouse; BD, 564372).

Luciferase assays

MEFs were pre-incubated for 4 h in medium containing 0.5% FBS and then treated with IL10 for the indicated times before lysing them to measure luciferase activity using the Promega Luciferase Assay System (E1500).

Assays with THP1 cells and BMDMs

THP1 cells were pre-treated with PMA (125 ng/ml; Sigma, P8139) for 48 h to promote their differentiation to macrophages, and then incubated in 1% FBS for 5 h before IL10 treatment. Wild-type and *Atg16l1*^{T300A} knock-in mice [20] were dissected and their tibias and femurs flushed with a 23 G syringe filled with cold culture medium containing 20% FBS to isolate bone marrow cells. Cells were then plated at a density of 2×10^6 cells/ml and treated with 20 ng/ml CSF1 for 6 days. Adherent cells were harvested at the end of the differentiation process using a cell scraper and plated in 20% FBS medium lacking CSF1 for 16 h. Next day, cells were incubated for 5 h in DMEM 1% FBS before IL10 and/or LPS (Invivogen, Tlrl-3pelps) treatment. Mice were maintained and euthanized following European regulations.

Quantitative PCR

Total RNA was isolated from BMDMs using the RNeasy Mini Kit (Qiagen, 74104) and used for quantitative PCR (qPCR) with the qPCR iTaq Universal SYBR Green One-Step kit (Bio-Rad, 1725150). Around 30–50 ng of total RNA was used as a template per qPCR reaction. Data were corrected against the results obtained for *Actb/Actin beta* or *Gapdh* (as control genes) to obtain fold variations of gene expression between control and treated cells following the $2^{-\Delta\Delta}C_T$ method [27]. Arbitrary measurements of mRNA abundance in all conditions were obtained by calculating the individual relative copy number (RCN) using internally-corrected $2^{-\Delta}C_T$ values as previously described [28]. Primers were selected with the PrimerBank Primer Search on-line tool (MGH, Harvard; https://pga.mgh.harvard.edu/primerbank/). Primer sequences were: mouse *Bcl3*: fw, 5' CCGGAGGCCCTTTACTACCA 3', rev, 5' GGAGTAGGGGTGAGTAGGCAG 3'; mouse *Tnf*: fw, 5' CCCTCACACTCAGATCATCTTCT 3', rev, 5' GCTACGACGTGGGCTACAG 3'; mouse *Actb/Actin beta*:

fw, 5' GGCTGTATTCCCCTCCATCG 3', rev, 5' CCAGTTGGTAACAATGCCATGT 3'; mouse *Gapdh*: fw, 5' AGGTCGGTGTGAACGGATTTG 3', rev, 5' TGTAGACCATGTAGTTGAGGTCA 3'.

Statistical analysis

Graphs shown in Figures 2D, 2G and 3D were generated using Excel and those in Figures 3E and 3F were generated using GraphPad Prism 7.04. In all cases the data represent mean -/+ standard deviation values obtained from the indicated number of experimental points (n). Statistical significance was established by calculating the P-values resulting from two-tailed Student's t-tests.

Acknowledgments

We thank Dr. Ramnik J. Xavier for providing the *Atg16l1*^{T300A} knock-in mice and members of the CIC for support. This work was funded by grants from the Ministerio de Ciencia e Innovación of the Spanish Government (Refs. SAF2017-88390-R and PID2020-114699RB-100), the Junta de Castilla y León local government (Ref. SA042P17), the Broad Medical Research Program (Crohn's and Colitis Foundation of America, CCFA; Ref. IBD-0369) and the Fundación Solórzano (Ref. FS/18-2014). The Centro de Investigación del Cáncer is supported by the Programa de Apoyo a Planes Estratégicos de Investigación de Estructuras de Investigación de Excelencia cofunded by the Castilla–León autonomous government and the European Regional Development Fund (CLC–2017–01). Additional funding comes from the Fondo Europeo de Desarrollo Regional (FEDER) program of the European Union. I.S.G. was supported by predoctoral fellowships from the Fundación Moraza and the Estrategia Regional de Investigación e Innovación (Junta de Castilla y León and FEDER; Ref. CLC-2017-01). R.V. and A.F. are the recipients of predoctoral contracts from the Junta de Castilla y León and the University of Salamanca, respectively. F.X.P holds a tenured position at the CSIC.

Disclosure statement

No potential conflict of interests was reported by the authors.

Funding

This work was supported by the Ministerio de Economía, Industria y Competitividad, Gobierno de España [SAF2017-88390-R, PID2020-114699RB-100]; Consejería de Educación, Junta de Castilla y León [SA042P17] and [CLC-2017-01]; Crohn's and Colitis Foundation of America [IBD-0369]; Fundación Solórzano (USAL) [FS/18-2014]"

References

[1] Bento CF, Renna M, Ghislat G, et al. Mammalian autophagy: how does it work? Annu Rev Biochem. 2016;85:685–713.
[2] Fujita N, Itoh T, Omori H, et al. The Atg16L complex specifies the site of LC3 lipidation for membrane biogenesis in autophagy. Mol Biol Cell. 2008;19:2092–2100.
[3] Mizushima N, Kuma A, Kobayashi Y, et al. Mouse Apg16L, a novel WD-repeat protein, targets to the autophagic isolation membrane with the Apg12-Apg5 conjugate. J Cell Sci. 2003;116:1679–1688.
[4] Fujita N, Saitoh T, Kageyama S, et al. Differential involvement of Atg16L1 in crohn disease and canonical autophagy: analysis of the organization of the Atg16L1 complex in fibroblasts. J Biol Chem. 2009;284:32602–32609.
[5] Boada-Romero E, Serramito-Gómez I, Sacristán MP, et al. The T300A Crohn's disease risk polymorphism impairs function of the WD40 domain of ATG16L1. Nat Commun. 2016;7:11821.
[6] Fletcher K, Ulferts R, Jacquin E, et al. The WD 40 domain of ATG 16L1 is required for its non-canonical role in lipidation of LC 3 at single membranes. EMBO J. 2018;37:1–17.
[7] Boada-Romero E, Letek M, Fleischer A, et al. TMEM59 defines a novel ATG16L1-binding motif that promotes local activation of LC3. EMBO J. 2013;32:566–582.
[8] Heckmann BL, Teubner BJW, Boada-Romero E, et al. Noncanonical function of an autophagy protein prevents spontaneous alzheimer's disease. Sci Adv. 2020;6:eabb9036.
[9] Ulferts R, Marcassa E, Timimi L, et al. Subtractive CRISPR screen identifies the ATG16L1/vacuolar ATPase axis as required for non-canonical LC3 lipidation. Cell Rep. 2021;37:109899.
[10] Xu Y, Zhou P, Cheng S, et al. A bacterial effector reveals the V-ATPase-ATG16L1 axis that initiates xenophagy. Cell. 2019;178:552–566.e20.
[11] Pimentel-Muiños FX, Boada-Romero E. Selective autophagy against membranous compartments: canonical and unconventional purposes and mechanisms. Autophagy. 2014;10:397–407.
[12] Slowicka K, Serramito-Gómez I, Boada-Romero E, et al. Physical and functional interaction between A20 and ATG16L1-WD40 domain in the control of intestinal homeostasis. Nat Commun. 2019;10:1834.
[13] Serramito-Gómez I, Boada-Romero E, Villamuera R, et al. Regulation of cytokine signaling through direct interaction between cytokine receptors and the ATG16L1 WD40 domain. Nat Commun. 2020;11:5919.
[14] Hampe J, Franke A, Rosenstiel P, et al. A genome-wide association scan of nonsynonymous SNPs identifies a susceptibility variant for Crohn disease in ATG16L1. Nat Genet. 2007;39:207–211.
[15] Rioux JD, Xavier RJ, Taylor KD, et al. Genome-wide association study identifies new susceptibility loci for Crohn disease and implicates autophagy in disease pathogenesis. Nat Genet. 2007;39:596–604.
[16] Khor B, Gardet A, Xavier RJ. Genetics and pathogenesis of inflammatory bowel disease. Nature. 2011;474:307–317.
[17] Cadwell K, Liu J, Brown SL, et al. A unique role for autophagy and Atg16L1 in paneth cells in murine and human intestine. Nature. 2008;456:259–263.
[18] Sorbara MT, Ellison LK, Ramjeet M, et al. The protein ATG16L1 suppresses inflammatory cytokines induced by the intracellular sensors Nod1 and Nod2 in an autophagy-independent manner. Immunity. 2013;39:858–873.
[19] Kuballa P, Huett A, Rioux JD, et al. Impaired autophagy of an intracellular pathogen induced by a crohn's disease associated ATG16L1 variant. PLoS One. 2008;3:3391.
[20] Lassen KG, Kuballa P, Conway KL, et al. Atg16L1 T300A variant decreases selective autophagy resulting in altered cytokine signaling and decreased antibacterial defense. Proc Natl Acad Sci U S A. 2014;111:7741–7746.
[21] Murthy A, Li Y, Peng I, et al. A Crohn's disease variant in Atg16l1 enhances its degradation by caspase 3. Nature. 2014;506:456–462.
[22] Shouval DS, Ouahed J, Biswas A, et al. Interleukin 10 receptor signaling: master regulator of intestinal mucosal homeostasis in mice and humans. Adv Immunol. 2014;122:177–210.
[23] Serramito-Gómez I, Boada-Romero E, Pimentel-Muiños FX. Unconventional autophagy mediated by the WD40 domain of ATG16L1 is derailed by the T300A Crohn disease risk polymorphism. Autophagy. 2016;12:2254–2255.
[24] Lystad AH, Carlsson SR, de la Ballina Lr, et al. Distinct functions of ATG16L1 isoforms in membrane binding and LC3B lipidation in autophagy-related processes. Nat Cell Biol. 2019;21:372–383.
[25] Messer JS, Murphy SF, Logsdon MF, et al. The crohn's disease: associated ATG16L1 variant and Salmonella invasion. BMJ Open. 2013;3:e002790.
[26] Conway KL, Kuballa P, Song JH, et al. Atg16l1 is required for autophagy in intestinal epithelial cells and protection of mice from Salmonella infection. Gastroenterology. 2013;145:1347–1357.
[27] Livak KJ, Schmittgen TD. Analysis of relative gene expression data using real-time quantitative PCR and the 2-ΔΔCT method. Methods. 2001;25:402–408.
[28] Gavrilin MA, Bouakl IJ, Knatz NL, et al. Internalization and phagosome escape required for francisella to induce human monocyte IL-1β processing and release. Proc Natl Acad Sci U S A. 2006;103:141–146.